available at www.sciencedirect.com

ScienceDirect

journal homepage: www.elsevier.com/locate/agrformet

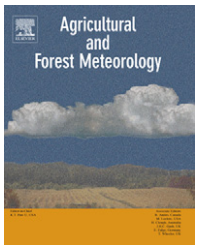

Evaporation of intercepted rainfall from isolated evergreen oak trees: Do the crowns behave as wet bulbs?

F.L. Pereira [a,e,*], J.H.C. Gash [b,c], J.S. David [d,e], F. Valente [d,e]

[a] Escola Superior Agrária, Instituto Politécnico de Castelo Branco, Quinta da Senhora de Mércules, 6001-909 Castelo Branco, Portugal
[b] Centre for Ecology and Hydrology, Wallingford OX10 8BB, United Kingdom
[c] VU University Amsterdam, Amsterdam 1081 HV, The Netherlands
[d] Instituto Superior de Agronomia, Universidade Técnica de Lisboa, Tapada da Ajuda, 1349-017 Lisboa, Portugal
[e] Centro de Estudos Florestais, Tapada da Ajuda, 1349-017 Lisboa, Portugal

ARTICLE INFO

Article history:
Received 15 July 2008
Received in revised form
8 October 2008
Accepted 21 October 2008

Keywords:
Evaporation
Rainfall interception
Isolated trees
Quercus ilex
Wet bulb temperature
Surface temperature

ABSTRACT

A new approach is suggested for estimating evaporation of intercepted rainfall from single trees in sparse forests. It is shown that, theoretically, the surface temperature of a wet tree crown will depend on the available energy and windspeed. But for a fully saturated canopy under rainy conditions, surface temperature will approach the wet bulb temperature when available energy tends to zero. This was confirmed experimentally from measurements of the radiation balance, aerodynamic conductance for water vapour and surface temperature on an isolated tree crown. Net radiation over a virtual cylindrical surface, enclosing the tree crown, was monitored by a set of radiometers positioned around that surface. Aerodynamic conductance for the tree crown was derived by scaling up measurements of leaf boundary layer conductance using the heated leaf replica method. Thermocouples were used to measure the average leaf surface temperature. Results showed that a fully wet single tree crown behaves like a wet bulb, allowing evaporation of intercepted rainfall to be estimated by a simple diffusion equation for water vapour, which is not restricted by the assumptions of one-dimensional transfer models usually used at the stand scale. Using this approach, mean evaporation rate from wet, saturated tree crowns was 0.27 or 0.30 mm h^{-1}, when surface temperature was taken equal to the air wet bulb temperature or estimated accounting for the available energy, respectively.

1. Introduction

Evaporation of rainfall intercepted by vegetation is usually an important part of an overall catchment water balance, especially in forested areas where it may represent 25–75% of total evaporation (David et al., 2005) and 8–9% (David et al., 2006) to 60% of gross rainfall (Forgeard et al., 1980), depending on the rainfall climate and forest type. Therefore, it is not surprising that many studies have been dedicated to measuring and modelling rainfall interception loss. The Rutter interception model (Rutter et al., 1971) was the first to explicitly represent interception as being driven by the evaporation rate from wet canopies, usually estimated by the Penman–Monteith equation. A simpler, storm-based analytical model was developed later by Gash (1979). This model can be used with average evaporation and rainfall rates

* *Corresponding author at*: Escola Superior Agrária, Instituto Politécnico de Castelo Branco, Quinta da Senhora de Mércules, 6001-909 Castelo Branco, Portugal. Tel.: +351 272339974/963221211; fax: +351 272339901.
E-mail address: flpereira@esa.ipcb.pt (F.L. Pereira).
0168-1923/$ – see front matter
doi:10.1016/j.agrformet.2008.10.013

during storms to estimate interception loss from daily rainfall data. In this case, mean evaporation rate is also usually estimated by the Penman–Monteith equation from meteorological data. However, the original formulations of both models failed to adequately predict interception loss from sparse forest canopies, and new, revised versions were proposed to overcome this (Gash et al., 1995; Valente et al., 1997). These revised models, which assume that evaporation is reduced in proportion to the canopy cover fraction, were successfully applied in open forests (Asdak et al., 1998; Carlyle-Moses and Price, 1999; Gash et al., 1995; Jackson, 2000; Valente et al., 1997). However, the use of the one-dimensional Penman–Monteith model may be questionable in spatially non-homogeneous vegetation such as very sparse forests. The research described in this paper is therefore directed at finding an alternative method of modelling evaporation under such conditions. Sparse forests are particularly important given their dominant distribution over dry and semi-arid areas where water resources are scarce (Stewart, 2004).

2. Theory

Dalton (1802) was the first to identify evaporation (E) as a diffusion process, driven by a humidity difference. The relationship can be written (see Gash and Shuttleworth, 2007) as

$$E = K(e_s - e_a) \tag{1}$$

where the coefficient K depends on windspeed, e_s is the saturated vapour pressure at the evaporating surface temperature and e_a represents the actual vapour pressure in the air above. For a saturated canopy, following Brutsaert (1991) and Monteith and Unsworth (2008), Eq. (1) can be given a more precise physical meaning by expressing it in an integrated form as

$$\lambda E = \frac{\rho_a c_p}{\gamma} g_{bV}[e_s(T_s) - e_a] \tag{2}$$

where λ is the latent heat of vaporization, ρ_a is air density, c_p is air specific heat at constant pressure, γ represents the psychrometric constant, g_{bV} is the aerodynamic conductance for water vapour integrated over the path between the surface of the leaves and the air layer adjacent to the tree crown, $e_s(T_s)$ is the saturation vapour pressure at surface temperature T_s and e_a represents the actual vapour pressure of the surrounding air.

Penman (1948) and later Monteith (1965) derived one-dimensional equations that combined Eq. (2) with the energy balance of an evaporating surface, assuming a complete canopy cover. These equations were based on the approximation that the curve relating the saturation vapour pressure to temperature is linear over the range between the surface and air temperatures, allowing surface temperature to be eliminated. Evaporation from vegetation could then be estimated using standard meteorological data measured at a single reference height.

This approach has been used for the estimation of the evaporation rate from a wet forest canopy in most of the previous physically based rainfall interception models. In the early modelling approaches, the forest canopy was represented as a single, uniform source for water vapour (see Rutter et al., 1971). Although this worked well for closed forests, it did not seem adequate for sparse canopies. Gash et al. (1995) and Valente et al. (1997) adapted closed-canopy interception models to sparse forests, considering the forest canopy and the open spaces between trees separately and treating each one of these components as an independent and continuous area. The evaporation rate from the wet tree canopy component (E_c) was considered the same as that for a closed forest, estimated by the Penman–Monteith equation. Since the under-strata evaporation was considered negligible, the evaporation from the overall sparse forest (E) was reduced in proportion to the canopy cover fraction (c) (whenever appropriate, the subscript c denotes an evaporation rate referenced to the covered area).

The rate of evaporation from a wet canopy is strongly influenced by the aerodynamic conductance. Commonly, this conductance has been approximated to the bulk aerodynamic conductance for momentum over the path between the height of the apparent sink for momentum and a reference level above the canopy. This bulk aerodynamic conductance is usually represented as a function of tree height and windspeed, irrespective of canopy cover fraction. Any effect of forest sparseness on turbulence and the consequent evaporation enhancement (Teklehaimanot et al., 1991) has been neglected. However, this is no longer appropriate when the sparseness of the canopy increases, and the trees behave as isolated units. In this case, windspeed at the tree crown level will become higher, the whole crown of each tree will tend to be subjected to the same meteorological conditions and all the leaves equally exposed to the free air stream. Under these conditions, the assumed exponential eddy and windspeed decay (e.g. Dolman, 1993; Hall, 2002; Shuttleworth and Wallace, 1985) characteristic of closed canopies will be greatly reduced, resulting in a much higher conductance affecting the water vapour flux from soil and under-strata (grasses and shrubs). In this case, the effect of under-strata on the overall aerodynamic conductance and evaporation can no longer be ignored and the evaporation rate from wet, isolated trees has to be evaluated separately, considering its dependence on the surrounding, rather than above-canopy, environmental conditions. An individual-tree approach will, therefore, be the most appropriate.

Eq. (2) could be used to estimate evaporation from the fully wet crown of an isolated tree, if its crown surface temperature was known. Following the suggestion by Alves et al. (2000), the combination of the latent and sensible heat flux equations with the energy balance of a single, isolated wet tree, allows the calculation of its surface temperature (hereafter and whenever necessary, subscripts *s,calc* and *s,meas* will be used to distinguish between calculated and measured surface temperature, respectively) as (see Appendix A):

$$T_{s,calc} = \frac{1}{\rho_a c_p} \frac{\gamma}{\Delta + \gamma} \frac{A}{g_{bV}} + T_w \tag{3}$$

where Δ is the slope of the saturation vapour pressure vs. temperature curve, A is the available energy per unit tree crown projected area and T_w is the wet bulb temperature of the air.

According to Eq. (3), tree crown surface temperature will tend to be higher than wet bulb temperature (i.e. $T_{s,calc} > T_w$), depending on available energy and windspeed. However, the temperature of a wet, saturated canopy should approach the wet bulb temperature when available energy tends to zero, as is often the case during rainfall/cloudy conditions. This is in agreement with theory (e.g. Monteith and Unsworth, 2008; Stewart and Thom, 1973), but also with some previous experimental results (e.g. Landsberg and Thom, 1971; Teklehaimanot and Jarvis, 1991). In this study we will test the hypothesis that surface temperature is sufficiently close to the wet bulb temperature (i.e. $T_s \approx T_w$) under rainy/cloudy conditions, to allow it to be used in Eq. (2) to estimate the average evaporation rate from wet, isolated tree crowns.

3. Site description

The study was carried out in a mixed oak woodland (*montado*) at the ''Herdade da Mitra'' - Mitra II field site (38°32′N, 8°00′W), University of Évora, some 15 km west of the city of Évora, in Southern Portugal. *Montados* (or *dehesas* in Spain) are savanna-type Mediterranean oak forests strongly influenced by human action and usually managed for agroforestry. Typically, *montados* have a forest stratum dominated by widely separated evergreen oaks (*Quercus* sp.) and an understorey of grass and shrubs commonly used for cattle grazing. The study site (hereafter referred to as Mitra II) was located in a holm oak (*Quercus ilex* ssp. *rotundifolia*) stand. The trees are sparsely distributed (see Fig. 1) in an area of flat terrain, with a density of about 30 trees ha^{-1}, a crown cover of ca. 21% (Carreiras et al., 2006) and an average tree height of 7.3 m (from a survey of nine trees in the experimental plot). Local climate is Mediterranean, with mild winters and hot, dry summers. Average annual rainfall is 665 mm, usually occurring from autumn to early spring (INMG, 1991). Further details of the site are given by Pereira et al. (2007).

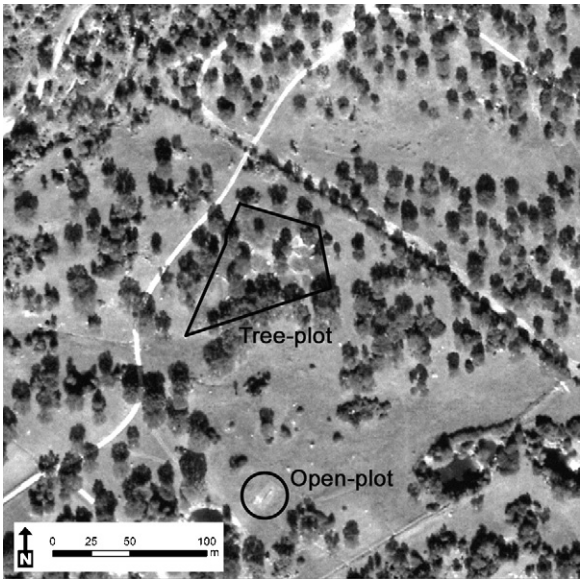

Fig. 1 – Aerial view of the Mitra II field site.

4. Methods

4.1. Experimental plots

Two experimental plots were set up at a distance of 150 m from one another at the Mitra II site. One of these plots (''Open-plot'' in Fig. 1) was in an open area and was used for gross rainfall measurement with a 0.2 mm tipping-bucket raingauge (Casella, Bedford, UK). The tipping-bucket measurements were totalised and stored every 10 min in a CR10X data-logger (Campbell Scientific, Shepshed, UK). The other plot was located inside the oak woodland (''Tree-plot'' in Fig. 1) and included nine *Q. ilex* trees. One tree was selected for the measurement of its radiation balance and another tree for the measurement of the other variables controlling evaporation (temperature and boundary layer conductance of leaves, wet and dry bulb temperatures and windspeed at crown level). Access to the tree crowns was provided by two metal towers, 6 and 7 m high. In a *Q. ilex* tree of a nearby identical *montado*, David et al. (2004) measured by destructive sampling the single tree leaf area index (L^*, $L^* = 2.6$), which was assumed to be representative for our site. Multiplying L^* by the crown projected area of each of the two sampled trees (radiation and evaporation), allowed their leaf area (L_A) to be estimated as 110 and 229 m^2, respectively.

4.2. Available energy

Following the methodology firstly described by Thorpe (1978), the net radiant energy received by the entire tree crown (Q_c) was evaluated as the total energy flux through an imaginary surface S, completely enclosing the crown. This energy flux can be determined as the integral of net radiation (R_n) at each point of the enclosing surface as

$$Q_c = \iint_S R_n \, dS$$

Since *Q. ilex* crowns are flat-topped, we assume S as a cylinder centred on the tree longitudinal axis, with a radius equal to the tree crown mean radius, a height corresponding to the crown depth and comprising three surfaces – a vertical cylindrical surface (S_1) and two circular surfaces (S_2 and S_3 at the bottom and top, respectively). The integral of R_n can therefore be expressed as

$$Q_c = \iint_{S_1} R_{n,1} \, dS_1 + \iint_{S_2} R_{n,2} \, dS_2 + \iint_{S_3} R_{n,3} \, dS_3$$

Using the procedure for calculating surface integrals given by Colley (1998) and assuming $R_{n,3}$ constant for any point of S_3, this equation can be expanded to

$$Q_c = c_r(z_h - z_c) \int_0^{2\pi} R_{n,1}(s) \, ds + \frac{c_r^2}{2} \int_0^{2\pi} R_{n,2}(s) \, ds + \pi c_r^2 R_{n,3} \quad (4)$$

where z_h is the tree height, z_c is the height of the crown base, c_r is the tree crown mean radius and s the angle of each point defining its position around the tree crown. Since the functions $R_{n,1}(s)$ and $R_{n,2}(s)$ are not known, Q_c was calculated numerically using the composite Simpson's rule (Allen and Isaacson, 1998). Numerical integration of Eq. (4) was based on point measurements of R_n representative of specific discrete

areas. Ideally, these should have been simultaneous measurements to avoid the variability of radiation in time, as can happen under partially clouded skies (McNaughton et al., 1992; Wünsche et al., 1995). However, this would have required a complex experimental setup for which the necessary resources were not available. To overcome this, a simple measuring device was built, consisting of a telescopic metallic rod held vertically by a stable tripod base. Three hemispherical net radiometers (NR Lite, Kipp & Zonen, Delft, The Netherlands) were mounted on the rod: two installed vertically to monitor R_n at the lateral surface (S_1) and one mounted horizontally up-side-down to monitor net radiation into the lower surface (S_2). A fourth identical sensor was installed in a horizontal, fixed position immediately above the tree crown, to measure R_n at the top surface (S_3). All the sensors were calibrated before the experiment.

To measure R_n on the vertical surface around the tree, the sensors on the telescopic rod were successively positioned at six equally spaced points encircling the tree. Measurements were made for 2 min at each point. In the following 2 min, the sensors were moved to a new position, with the procedure repeated until measurements had been made in all the six positions. A measuring cycle thus lasted for a total of 22 min. R_n was sampled every 6 s and 2 min averages recorded by a CR10X data-logger (Campbell Scientific, Shepshed, UK). Using this procedure, Q_c was sampled intermittently on 8 days with different weather conditions during the first 3 months of 2006. Measurements were considered acceptable only when the radiation at the top of the crown was uniformly stable during the monitoring cycle. During the same period night-time measurements of R_n were also made, on 43 non-consecutive nights, but with the net radiometers at fixed positions. Measured values were extrapolated to the other trees with the assumption that Q_c was proportional to the size of the enclosing surface.

The storage term (J) of available energy refers to the rate of change of energy stored physically and biochemically in the vegetation and in the surrounding air. J can thus be considered the sum of

$$J = J_H + J_V + J_{veg} + J_{Ph}$$

where J_H, J_V, J_{veg} and J_{Ph} are, respectively, the rate of change in the sensible and latent heat contents of the air surrounding the tree, the rate of change in the heat stored in the tree biomass and the rate of energy being stored biochemically in the tree. These components of J were estimated for the reference volume of the enclosing cylinder previously defined for the estimation of Q_c. Given that this cylinder has a cross-section equal to the tree crown projected area, those components were expressed on a crown projected area basis. Since trees have a high percentage of their biomass concentrated in the trunk and branches, J_{veg} can be further separated into a term that represents energy stored in the large woody parts of the tree (J_{tr}) and another representing energy stored in leaves and twigs (J_{crown}). These two components of J_{veg} have different thermal properties, with the temperature of leaves closely in phase with air temperature (Moore and Fisch, 1986), while trunk temperature shows a phase lag in relation to changing air temperature.

Using temperature and humidity measurements taken at the Tree-plot, J_H and J_V were calculated as suggested by Thom (1975) but using a finite difference approximation

$$J_H = \rho_a c_p \frac{\Delta\overline{T}}{\Delta t}(z_h - z_c)$$

and

$$J_V = \rho_a \lambda \frac{\Delta\overline{q}}{\Delta t}(z_h - z_c)$$

where $\Delta\overline{T}$ and $\Delta\overline{q}$ are the change in mean air temperature and humidity, respectively, $z_h - z_c$ is the height of the air column that surrounds the tree crown and Δt is a 10 min interval.

Assuming that the density ($\rho_{veg(crown)}$), specific heat ($c_{veg(crown)}$) and temperature variation of leaves are all independent of height and that tree foliage is in phase with air temperature, J_{crown} was estimated as

$$J_{crown} = \rho_{veg(crown)} c_{veg(crown)} \frac{\Delta\overline{T}}{\Delta t}(z_h - z_c)$$

The rate of energy storage in the trunk and branches (J_{tr}) was estimated following the procedure described by Gash et al. (1999). J_{veg} was estimated as the sum of J_{crown} and J_{tr}.

Following Gash et al. (1999), the energy storage due to photosynthesis was estimated as being $-1\ \mathrm{W\ m^{-2}}$ during the night and the greater of $5\ \mathrm{W\ m^{-2}}$ or $0.02R_n$ during the day (Thom, 1975).

The net radiation flux expressed per unit tree crown projected area (Q) is

$$Q = \frac{Q_c}{\pi c_r^2}$$

and the available energy per unit of crown projected area is then given by

$$A = Q - J$$

4.3. *Leaf boundary layer conductance*

From 9 November 2005 to 31 January 2006 leaf boundary layer conductance for convective heat transfer (g_{lH}) was measured using the heated leaf replica method (Brenner and Jarvis, 1995). According to this method, g_{lH} can be determined from the temperature difference between two identical metal leaf replicas, one unheated and the other heated, as

$$g_{lH} = \frac{1}{\rho_a c_p}\left(\frac{P_e}{T_{sh} - T_{su}} - 4\varepsilon\sigma T_{su}^3\right) \quad (5)$$

where σ is the Stefan–Boltzmann constant, ε is the emissivity of the replicas' surfaces, T_{sh} and T_{su} are the surface temperatures of the heated and unheated replicas, respectively, and P_e is the power supplied to the heated replica, calculated from

$$P_e = \frac{i^2 r}{S_t}$$

where i represents the current in the electrical circuit, r is the resistance of the heating element and S_t is the total surface area of the replica.

Three pairs of replicas were constructed. Each pair was made in the shape of the natural leaves but in different sizes to reproduce sun-lit (27 mm × 17 mm) and shaded (39 mm × 26 mm) leaves, as well as leaves with an intermediate dimension (34 mm × 19 mm). Leaf replicas were assembled using two similar brass plates. The heating element was an insulated constantan wire (OMEGA Engineering Ltd., Manchester, UK) with a 10 ohm resistance inserted between the plates before they were bonded together with epoxy adhesive. Both T_{sh} and T_{su} were measured using type-T thermocouples (OMEGA Engineering Ltd., Manchester, UK), 0.25 mm in diameter, attached to the lower surfaces of the replicas with aluminium foil. All the replicas were polished to ensure a high reflectance and a low emissivity and then mounted on a 140 mm × 165 mm frame. Using a universal joint, this frame was positioned next to the tree crown at 5.2 m height. During the first month, measurements were taken with the replicas at a 40° inclination and subsequently in a horizontal position. Measurements of replica surface temperature and voltage drop were made at a frequency of 0.167 Hz, and 10 min averages were recorded on a CR10X datalogger (Campbell Scientific, Shepshed, UK).

Data quality was guaranteed by filtering measurements according to the criteria used by Smith et al. (1997a) and considering only measurements when the difference between the temperature of unheated replicas and dew point temperature was greater than 1.0 °C. From these measurements, g_{lH} was determined by Eq. (5) and converted to a water vapour conductance (g_{lV}) taking into consideration the relation between air thermal conductivity and water vapour diffusivity in air (1.08 or 1.00 depending on whether air flow in the leaf boundary layer is laminar or turbulent (Grace, 1983; Jones, 1992)).

Bulk aerodynamic conductance for the tree crown (g_{bV}) was scaled up from leaf boundary layer conductances, based on the assumption that all the conductances of individual leaves act in parallel. Accordingly, g_{bV} was calculated as

$$g_{bV} = \overline{g_{lV}} L^* \quad (6)$$

where $\overline{g_{lV}}$ is the mean leaf boundary layer conductance for water vapour.

With the objective of assessing the possibility of using simple theoretical relationships to evaluate leaf boundary layer conductance, the measured values were compared to estimates given by formulae derived from the heat transfer theory (see Monteith and Unsworth, 2008), usually referred to as ''engineering formulae''. The theoretical formula used was derived following Monteith and Unsworth (2008) and Schuepp (1993), assuming: (a) forced convection to be the dominant transfer process, (b) a laminar leaf boundary layer and (c) leaves represented as flat plates with an average characteristic dimension of 21 mm. Calculated leaf conductance for heat transfer was converted to that for water vapour, and scaled up to the whole tree, as previously described.

4.4. *Leaf temperature, wet and dry bulb temperatures and windspeed at crown level*

T_s was taken as the average temperature measured by 12 type-T thermocouples (OMEGA Engineering Ltd., Manchester, UK) placed over the upper surface of leaves and kept in position using thermal glue. In order to get a representative estimate for the temperature of the entire crown, thermocouples were placed on both outside, exposed leaves, as well as on inside, sheltered leaves. Two aspirated psychrometers (Wright et al., 1992) were installed on one of the towers at a height of 4.2 m, one positioned outside and the other inside the canopy. One anemometer (type A100R, Vector Instruments, Rhyl, UK) was also installed at 4.8 m height, outside the tree crown. Data from all these instruments were sampled at 10 s intervals and averages recorded every 10 min on a CR10X data-logger (Campbell Scientific, Shepshed, UK). Data were collected between March 2005 and January 2006. Unreliable data were discarded, for example when the thermocouples became detached from the leaves or when leaves were damaged.

4.5. *Average evaporation rate from wet, saturated tree crowns*

The evaporation rate (E_c) was estimated by Eq. (2) in two different ways: one considering the crown surface temperature (T_s) equal to the air wet bulb temperature ($E_c(T_{s,w})$) and the other with T_s calculated using Eq. (3) ($E_c(T_{s,calc})$). Following Gash (1979), tree crowns were considered saturated for all hours when gross rainfall rate equalled or exceeded 0.4 mm h^{-1} (two bucket tips). The evaporation rates were averaged for all these hourly time intervals, providing estimates for the average evaporation rates under saturated canopy conditions ($\overline{E}_c(T_{s,w})$ and $\overline{E}_c(T_{s,calc})$).

5. Results and discussion

5.1. *Available energy*

The input of total radiative energy to the tree was dominated by the R_n component at the tree top which, on average, accounted for about 72% of Q_c. Fig. 2 shows a good linear fit between Q_c (W) and R_n (W m^{-2}) measured above the crown ($Q_c = 62.0R_n + 39.6$, $R^2 = 0.97$). Given the dependence of net radiation upon short wave radiation, Q_c (W) also showed a

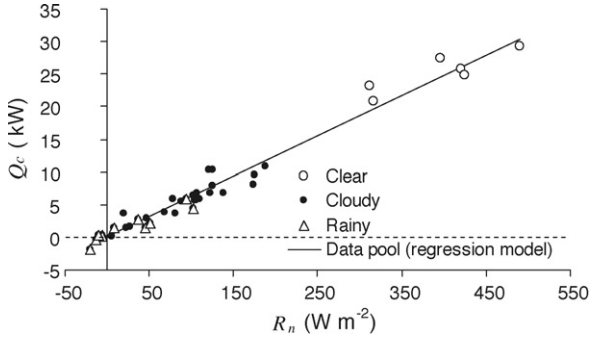

Fig. 2 – Relationship between Q_c and R_n (at the canopy top, averaged over the measurement periods) for different weather conditions. The linear regression model for the entire data set (all weather conditions) is also represented (full line).

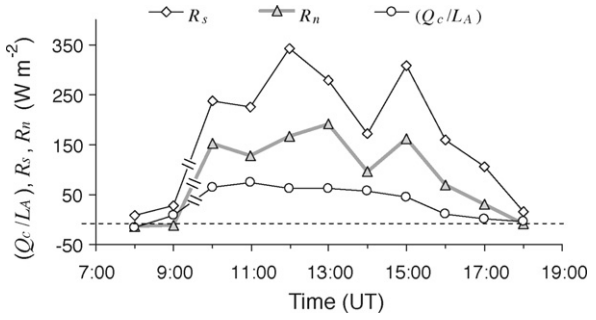

Fig. 3 – R_s, R_n and ratio of total energy to leaf area (Q_c/L_A) for an isolated tree under cloudy/rainy conditions. Measurements started on 3 March 2006 and ended on 4 March 2006. Values of R_s and R_n represent hourly averages.

strong linear response to R_s (W m^{-2}) ($Q_c = 41.8R_s - 1.53 \times 10^3$, $R^2 = 0.95$).

Fig. 2 suggests a dependence on weather conditions with the occurrence of rain seeming to cause a small decrease in Q_c in comparison to clear sky conditions. However, these differences might possibly be just a subtle indication that these relationships are not linear, as suggested by Angelocci et al. (2004), corresponding instead to different parts of a more general sigmoid trend.

Fig. 3 shows the data collected during a composite day comprising 10:00 to 18:00 h on 3 March 2006 and 08:00 to 09:00 h on the following day. For this whole period the canopy was wet. It can been seen that solar and net radiation are low and the daily time-course of (Q_c/L_A) follows closely those of R_s and R_n, with a maximum of only about 75 W m^{-2}, which is similar to that measured by McNaughton et al. (1992) for an apple tree, under cloudy weather.

During day-time, short wave radiation, direct or diffuse, provides the most important contribution to R_n (Ross, 1975) but depends on the transparency of the atmosphere and on the apparent sun's position relative to the measuring point (Beer, 1990). These are the main factors that account for the strong spatial and temporal variability that can affect R_n through the day. However, during the night and in the absence of short wave radiation, R_n becomes spatially homogeneous and its variation around the crown of an isolated tree is significantly reduced (Angelocci et al., 2004).

This was confirmed by our night-time measurements with the fixed position sensors, which showed that fluxes of net radiation in the lateral and inferior surfaces varied little during the night (Fig. 4a), being practically independent from the flux at the top (Fig. 4b). It thus seems reasonable to assume that these measurements represent well the R_n fluxes around the tree and, accordingly, they were used to calculate Q_c during the night. Then, a relationship between Q_c and R_n measured above the tree crown was established, allowing Q_c to be estimated whenever R_n measurements are available. Combining this regression equation with the one obtained for day-time periods it is then possible to estimate Q_c for a complete day using

$$\begin{cases} Q_c = 62.0R_n + 39.6, & R_s > 0 \\ Q_c = 71.7R_n + 138.2, & R_s = 0 \end{cases}$$

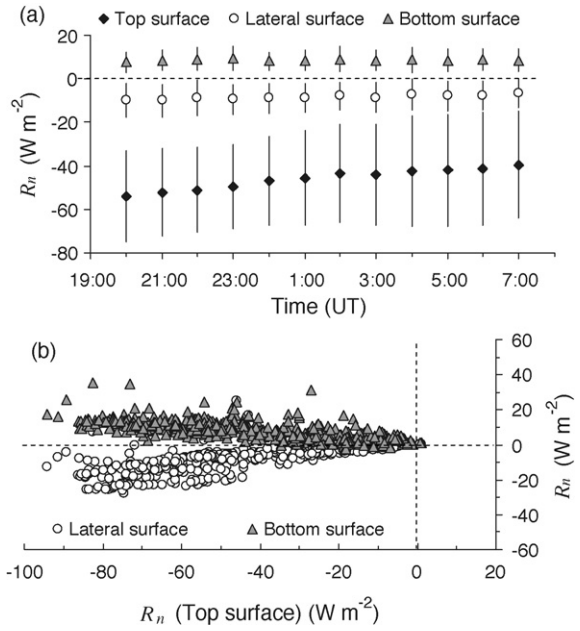

Fig. 4 – (a) Night-time variation of net radiation received at each of the surfaces enclosing the tree crown (for each hour, net radiation values correspond to the averages of all measurements made in study period and vertical bars represent the standard deviation). (b) Night-time relationship between R_n at the lateral and inferior enclosing surfaces and net radiation above the crown of an isolated tree.

As expected, Q follows a daily cycle with negative night-time values and a positive peak in the middle of the day (Fig. 5). The average hourly Q value over the entire measuring period, under cloudy/rainy conditions corresponding to saturated canopy, was low (about −7 W m^{-2}), with night and day-time Q hourly averages of approximately −55 W m^{-2} and 40 W m^{-2}, respectively.

When computed for periods of complete canopy saturation, J is almost constant over the day and very close to zero (−0.10 W m^{-2} on average) representing, therefore, a minor contribution to A (Fig. 5), confirming the observations made by Smith et al. (1997b) for trees in windbreaks in the Sahel.

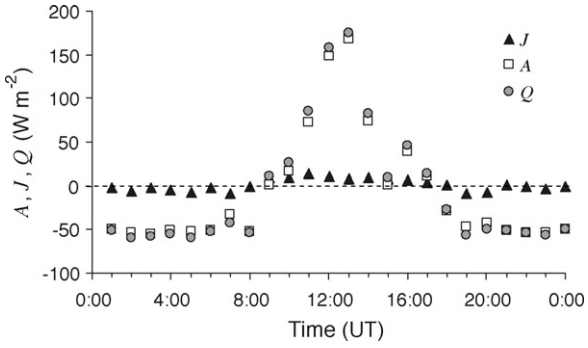

Fig. 5 – Daily cycle of J, Q and of available energy (A) for an isolated tree under saturated canopy conditions (plotted values are hourly averages).

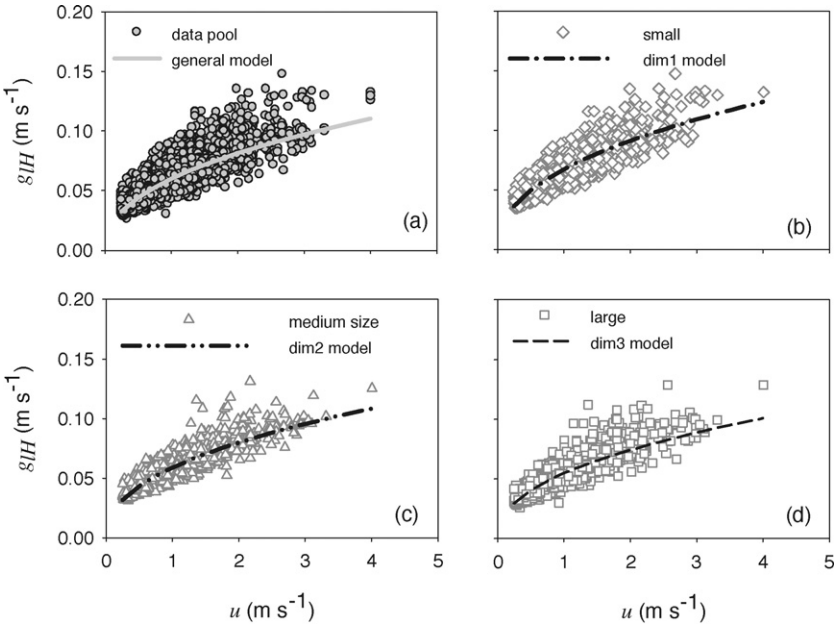

Fig. 6 – Scatter plots of g_{lH} against windspeed (u) for the complete data pool (a) and for data represented according to leaf dimension: small sun-lit leaves (dim 1) (b), intermediate size leaves (dim 2) (c) and larger shadowed leaves (dim 3) (d). The respective regression models are also shown.

5.2. *Aerodynamic conductance*

Under field conditions, measured g_{lH} values ranged between 0.025 and 0.150 m s^{-1} for windspeeds from 0.3 to 4.0 m s^{-1} (Fig. 6a). These values are relatively high, mostly because of the reduced thickness of the leaf boundary layer (lbl) determined by the small dimensions of the leaves, but are comparable to those observed in leaves of similar size (Brenner and Jarvis, 1995; Domingo et al., 1996; Smith et al., 1997a). However, they are considerably higher than those for larger leaves (Daudet et al., 1999; Grace et al., 1980; Grantz and Vaughn, 1999; Stokes et al., 2006; Thorpe and Butler, 1977). Although some previous studies (Landsberg and Powell, 1973; Landsberg and Thom, 1971; Michaletz and Johnson, 2006) suggested that positioning the replicas at the edge of the canopy might contribute to higher values of g_{lH}, results from Chen et al. (1988b) showed that the enhancement of g_{lH} caused by exposing the leaf replicas in the free air stream is not significant. The influence of leaf size and inclination on leaf boundary layer conductance can be further conditioned by leaf alignment relative to air flow. This additional influence results from changes in leaf characteristic dimension with wind direction (Grace, 1983), which also influences the effect of leaf inclination (Chen et al., 1988a,b; Schuepp, 1993; Smith et al., 1997a). To evaluate the importance of wind direction on the relationship between g_{lH} and windspeed, field measurements were divided into two data subsets corresponding to wind direction aligned with the long or short axis of leaves.

Since the theoretical relationship between g_{lH} and windspeed has the form $g_{lH} = au^b$, original values were transformed to allow the use of linear models of the type $\ln(g_{lH}) = \ln(a) + b\ln(u)$. Statistical analysis was performed according to the methodology described by Kutner et al. (2005), using the R software (R Development Core Team, 2007). Firstly, the above linear regression was calculated for the complete data pool (*general model*) as shown in Fig. 6a; secondly, linear regressions were calculated for each possible combination of dimension, inclination and alignment (*fully-differentiated model*); and finally, linear regressions were calculated separating the data according to leaf dimension (*dimension-differentiated model*). Although statistically different, the fully-differentiated and the dimension-differentiated models showed nearly identical predictive capacity (R^2 of 0.82 and 0.80, respectively). The use of the latter was preferred due to its greater simplicity. Fitted curves for the dimension-differentiated model are shown in Fig. 6b–d.

Results show that, independent of their alignment or inclination, sun-lit leaves have larger conductances than shaded ones. This is mostly a consequence of the smaller dimensions of sun leaves, although a minor influence may also be exerted by the structure of the canopy and the way it determines leaf microclimate (Stokes et al., 2006). For scaling up lbl conductances estimated with the dimension-differentiated model to the whole tree, the distribution of leaf area per leaf dimension class should, however, be known, which was not the case in the present study. Under these circumstances, lbl conductance was estimated simply from windspeed, regardless of dimension, alignment or inclination of leaves, using the overall relationship for the entire data pool ($R^2 = 0.72$) shown in Fig. 6a

$$g_{lH} = 0.06u^{0.441} \quad (7)$$

Considering that boundary layers of leaves are typically laminar, conductances for heat transfer were converted to water vapour conductances using $g_{lV} = 1.08g_{lH}$. Although measurements of g_{lH} were taken only at one level in the canopy they should still represent adequately conductances of the entire

foliage since, for open and exposed tree crowns, lbl conductances do not seem to vary much through the depth of the tree crown (Herbst et al., 2006). This allowed Eq. (6) to be used to scale-up the leaf boundary layer conductance to the bulk aerodynamic conductance for the entire tree crown (g_{bV}) which could then be expressed as $g_{bV} = 0.16u^{0.441}$.

An analogous relationship for g_{bV} based on theoretical engineering formulae was derived as described in Section 4.3: $g_{bV} = 0.12u^{0.5}$. When estimates given by this theoretical formula were compared with the experimental relationship, it was found that the average ratio between measured and estimated conductance was about 1.3. This value is within the usual range of variation reported for that ratio: 1.25–1.5 (Schuepp, 1993). If estimates of g_{bV} based on the engineering formulae are multiplied by this factor and plotted together with the experimental regression model, an almost perfect match between both lines is obtained (Fig. 7). This means that the estimation of the tree bulk aerodynamic conductance can be further simplified by using a practical procedure based on average leaf characteristic dimension and windspeed at the crown level.

5.3. *Canopy surface temperature during rainfall*

353 periods of completely wet canopy were selected from the 10 min data, using the criterion that rainfall occurred on each of the selected 10 min intervals and that rainfall in the previous hour was equal to, or greater than, 0.8 mm. In all time intervals meeting the above criterion, measured surface temperature ($T_{s,meas}$) closely matched the wet bulb temperature (T_w) observed next to the tree crown.

Fig. 8 illustrates a typical rainy period. In the initial phase of a storm, when the tree crown is not fully wetted, or when it starts to dry after rainfall has ceased, it can be seen that the available energy is usually higher. This extra energy warms up the canopy, increasing the difference between $T_{s,meas}$ and T_w. At the same time, variability of the average canopy temperature also increases as a consequence of the partial drying of the crown resulting from differences in exposure to both radiation and wind amongst individual leaves (Fig. 8). The closeness between canopy temperature and T_w becomes more

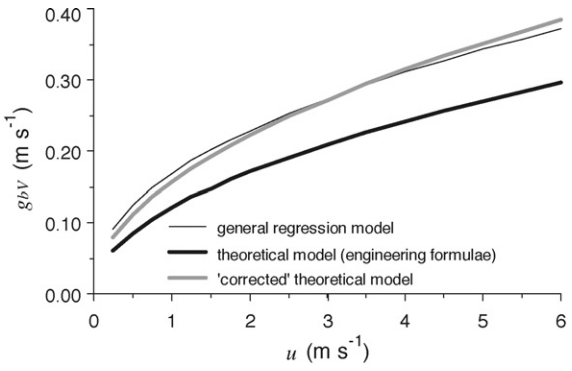

Fig. 7 – Bulk tree crown aerodynamic conductance for water vapour: experimental relationship (black thin line), theoretical engineering formula (black thick line) and theoretical relationship "corrected" by a factor of 1.3 (grey thick line).

evident when plotting T_w against $T_{s,meas}$ (Fig. 9) for all the 10 min intervals when the canopy was completely wet. Fig. 9 reveals a nearly 1:1 relationship. Fig. 10 shows the frequency distribution of $(T_{s,meas} - T_w)$. Considering that instrumental errors are likely to be in the range ±0.1 °C (Wright et al., 1992), the mean difference $\overline{(T_{s,meas} - T_w)} = 0.06$ °C is comparable with the instrumental error, with more than 75% of the values of this difference being within the range ±0.1 °C. We believe that the closeness of the tree crowns surface temperature to T_w is strongly influenced by the high values of g_{bV}, which result from the complete exposure of the crowns to the air stream. This exposure reduces the mutual sheltering effect found in denser canopies and allows the water on the leaf surfaces to approach the wet bulb temperature. Interestingly, during the occurrence of rainfall, the average windspeed observed by the anemometer adjacent to the tree crowns was 4 m s^{-1}, which is just above the threshold of 3 m s^{-1} over which a wet bulb thermometer is considered to be fully aspirated (Bindon, 1965).

As far as we are aware, this is the first study specifically designed to measure the canopy surface temperature of an isolated tree during periods of precipitation. Several previous studies have been carried out to directly evaluate evaporation rates from artificially wetted leaves, shoots or trees in the course of which surface temperature was also measured. However, these studies were, in general, made under good weather conditions and, thus, with higher radiation levels. In spite of this important difference, all studies tend to confirm that, when completely wet, the surface temperature of a tree crown gets very close to the wet bulb temperature of the adjacent air. For example, Landsberg and Thom (1971) found indistinguishable differences between the temperature of wetted needles/shoots and the air wet bulb temperature, when trying to determine transfer coefficients for water vapour in the controlled environmental conditions of a wind tunnel. Later on, in a study using the hanging-tree method to directly measure evaporation rate from a single tree, Teklehaimanot and Jarvis (1991) reported that surface temperature over the entire tree crown varied by no more than 0.5 °C after the tree was artificially wetted. This suggests that, when saturated, the canopy of an isolated tree has a homogeneous surface temperature, consistent with our assumption that the surface temperature of the entire wet tree crown can be adequately calculated as the average leaf temperature. Furthermore, it should be borne in mind that Teklehaimanot and Jarvis's measurements were made under dry conditions when the energy input was certainly several times higher than that to be expected under rain. Probably, their observed maximum 0.5 °C temperature difference over the tree crown would not be reached if measurements were made during the occurrence of rainfall.

More recently, Smith et al. (1997a) studying the aerodynamic conductances of trees in windbreaks also observed that on wetting the surface temperature of artificially wetted trees sharply declined, but remained higher than wet bulb temperature by 1.5–3.0 °C. However, this experiment was performed in the Sahel at high radiation flux densities. Under these circumstances, the contribution of radiation to warming up the canopy becomes significant and, according to Eq. (3), surface temperature should remain above T_w. We used Eq. (3) to simulate the results of Smith et al. (1997a). Assuming, from

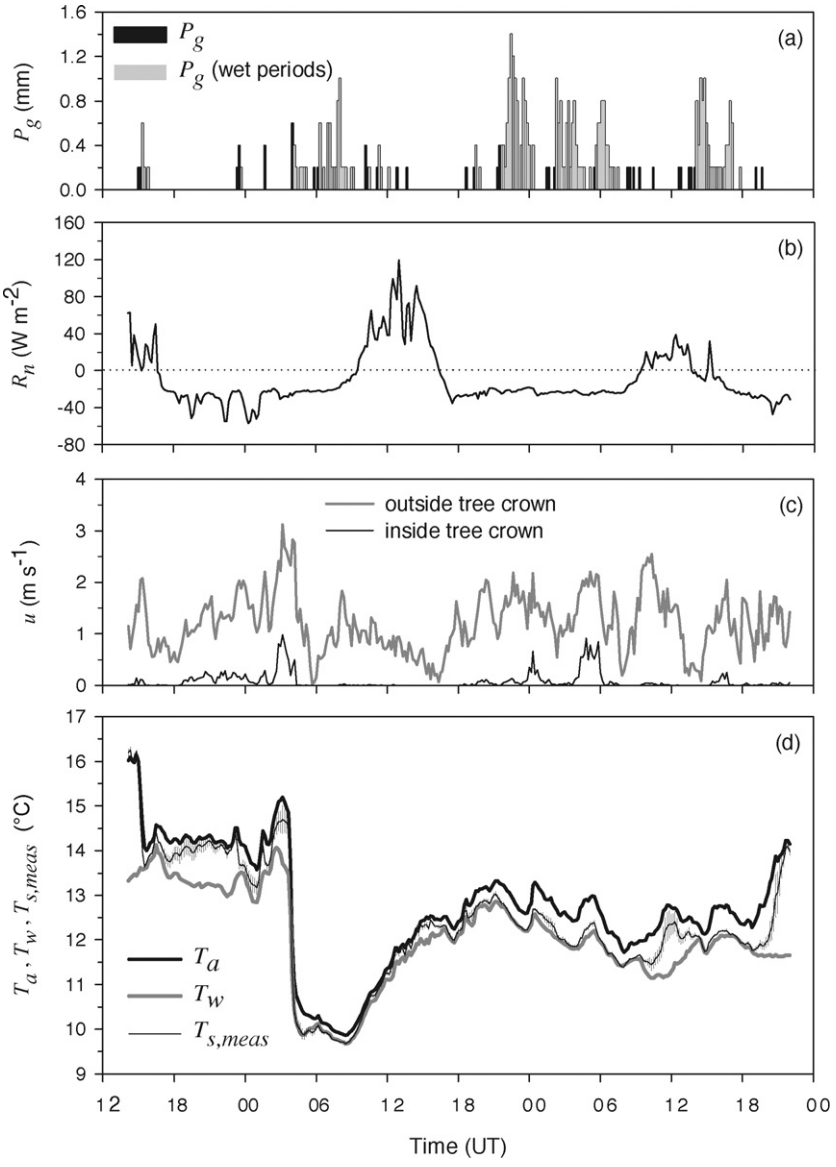

Fig. 8 – (a) Gross rainfall (P_g), (b) net radiation at the top of the tree crown (R_n) and (c) windspeed (u) both inside and outside the crown. (d) Air (T_a), wet bulb (T_w) and measured tree crown surface ($T_{s,meas}$) temperatures during a period of discontinuous precipitation. Vertical bars along the tree crown temperature curve represent the standard deviation. Periods of complete canopy saturation are identified by the light grey rainfall bars.

Smith et al. (1997b), $A = R_n \in [1700, 2000]$ W m^{-1} and, from Smith et al. (1997a), $u \in [2.0, 3.5]$ m s^{-1} and dry and wet bulb temperatures equal to 35 and 24 °C respectively, $T_{s,calc}$ given by Eq. (3) was in the range of 25.7–27.2 °C, i.e. 1.7–3.2 °C higher than T_w, in agreement with their findings given above.

Further confirmation for the validity of Eq. (3) is shown in Fig. 11 where tree crown surface temperature ($T_{s,calc}$) estimated by Eq. (3) using A and g_{bV} (calculated as described in Sections 4.2 and 4.3, respectively) is plotted against $T_{s,meas}$, for periods of completely saturated canopy. It can be seen that there is very good agreement between the two, showing the adequacy of Eq. (3) to represent the surface temperature of wet vegetation under low levels of radiation. As illustrated in Fig. 3 and discussed in Section 5.1, such low levels of radiation are typically found during rainfall. Thus, Eq. (3) seems adequate to estimate the surface temperature of a wet canopy, both for high and low radiation levels.

5.4. *Estimating average evaporation rates from wet, saturated crowns*

Estimated average wet canopy evaporation rate ($\overline{E}_c$) was 0.27 mm h^{-1} or 0.30 mm h^{-1}, when canopy surface temperature was considered equal to the air wet bulb temperature ($\overline{E}_c(T_{s,w})$) or when calculated by Eq. (3) ($\overline{E}_c(T_{s,calc})$), respectively. These values are within the normal range of reported values for $\overline{E}_c$ (e.g. Gash et al., 1995; Lankreijer et al., 1993; Lloyd et al., 1988; Rutter et al., 1971; Valente et al., 1997), which have been found to be rather conservative in forests, irrespective of climate type (David et al., 2005). Given the generally low levels

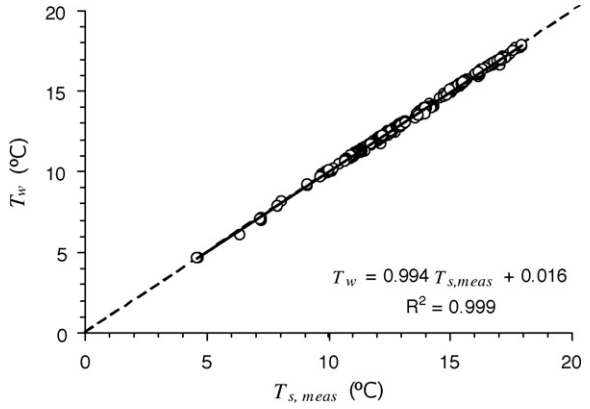

Fig. 9 – Wet bulb temperature (T_w) against measured surface canopy temperature ($T_{s,meas}$) for periods of completely saturated canopy. Dashed line corresponds to the 1:1 line, while the full line represents the linear regression model adjusted to plotted data.

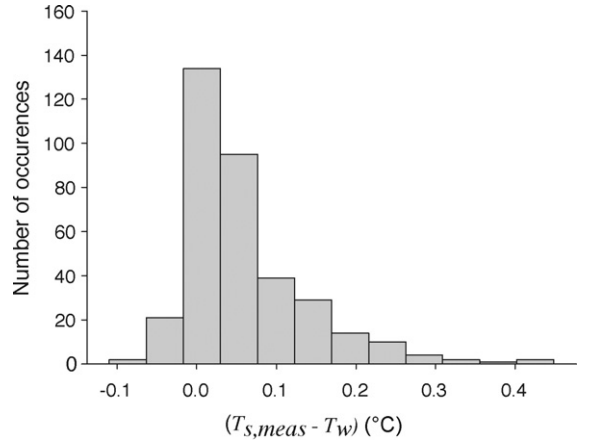

Fig. 10 – Histogram for the difference between measured surface temperature ($T_{s,meas}$) and T_w when the canopy was fully saturated.

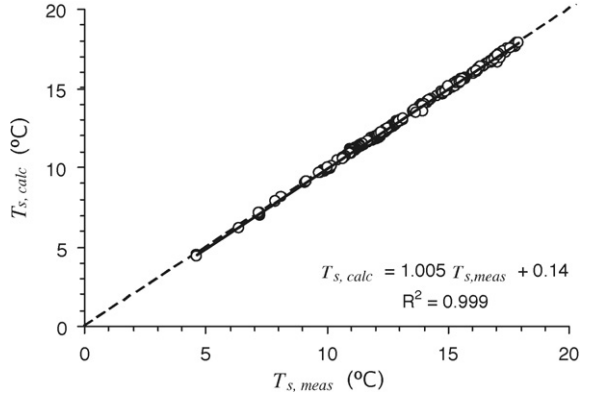

Fig. 11 – Calculated temperature (using Eq. (3)) for canopy surface ($T_{s,calc}$) against measured surface temperature ($T_{s,meas}$) for periods of completely saturated canopy. Dashed line corresponds to the 1:1 line, while the full line represents the linear regression model adjusted to plotted data.

of available energy during the occurrence of rainfall, it is not surprising that these two estimates are quite similar. The small difference between them shows that the rate of evaporation from wet, isolated crowns can be accurately estimated considering the approximation $T_s \approx T_w$, without needing the use of the more complex and data-demanding method that accounts for the available energy.

The $\overline{E}_c$ estimates obtained here are validated in a complementary study through their use in a rainfall interception model that was successfully tested against field observations (see Pereira et al., 2009).

6. Concluding remarks

For a wide range of climatic conditions, rainfall is associated with cloudy weather and low radiation energy input, allowing the assumption that available energy is negligible and $T_s = T_w$. This leads to the possibility of using Eq. (2) as a generally applicable, physically based predictive model for estimating evaporation from wet, isolated tree crowns, removing the need for radiation measurements, which are problematic for isolated trees.

Recent research into savanna-type sparse forests has favoured the application of scaling up the evaporation from individual trees rather than attempting to estimate evaporation from the landscape as a whole. For example, David et al. (2004, 2006) adopted a tree-based approach for measuring evaporation in a sparse evergreen oak woodland, using sapflow to measure transpiration and adopting a whole tree approach to measure rainfall interception. The tree-based approach might also be preferred for modelling evaporation from sparse forest, because in contrast to the Penman–Monteith model, it makes no assumptions about horizontal homogeneity. Using Eq. (2) as suggested above would be consistent with such a tree-based approach.

Acknowledgments

The authors thank the University of Évora for permission to work at the ''Herdade da Mitra'' field site. This study was supported by research project SAPIENS/FCT NO. POCTI/AGG/39220/2001 funded by the Fundação para a Ciência e Tecnologia. Funding was also provided by the Conselho de Reitores das Universidades Portuguesas and the British Council under the Treaty of Windsor Programme 2007/08 – U27. The authors are also grateful to Paulo Rocha Monteiro for his help in the construction and installation of several instruments, as well as for his collaboration in field work.

Appendix A. Surface temperature of the saturated crown of an isolated tree

The energy balance for a saturated tree crown can be expressed as

$$A = \lambda E + H \tag{A.1}$$

where A represents the tree available energy, λE and H are, respectively, the latent and sensible heat fluxes to the adjacent

air, all expressed per unit tree crown projected area. λE and H are given by

$$\lambda E = \frac{\rho_a c_p}{\gamma} g_{bV}[e_s(T_s) - e_a] \quad (A.2)$$

and

$$H = \rho_a c_p g_{bH}[T_s - T_a] \quad (A.3)$$

where ρ_a and c_p are, respectively, the air density and its specific heat at constant pressure, γ represents the psychrometric constant, T_a is the air temperature, $e_s(T_s)$ is the saturation vapour pressure at the tree crown surface temperature (T_s) and e_a is the actual vapour pressure of air; g_{bV} and g_{bH} are, respectively, the aerodynamic conductances for water vapour and sensible heat, assumed to be approximately equal and hereafter represented as g_b.

Substituting Eqs. (A.2) and (A.3) into Eq. (A.1) gives

$$A = \frac{\rho_a c_p}{\gamma} g_b[e_s(T_s) - e_a] + \rho_a c_p g_b[T_s - T_a] \quad (A.4)$$

Following Penman (1948) we introduce the approximation

$$e_s(T_s) \approx \Delta(T_s - T_a) + e_s(T_a) \quad (A.5)$$

and Alves et al. (2000)

$$e_s(T_a) - e_s(T_w) \approx \Delta(T_a - T_w) \quad (A.6)$$

where T_w is the air wet bulb temperature and Δ represents the slope of the linearised relationship between saturation vapour pressure and temperature, assumed to be valid over the temperature ranges in both Eqs. (A.5) and (A.6). Eq. (A.4) can then be rearranged as

$$\frac{A}{g_b} = \frac{\rho_a c_p}{\gamma}[\Delta(T_s - T_a) + e_s(T_a) - e_a + \gamma(T_s - T_a)] \quad (A.7)$$

Rearranging again and substituting for e_a using the wet bulb equation $e_a = e_s(T_w) - \gamma(T_a - T_w)$ Eq. (A.7) becomes

$$\frac{A}{g_b} = \frac{\rho_a c_p}{\gamma}[(\Delta + \gamma)(T_s - T_a) + e_s(T_a) - e_s(T_w) + \gamma(T_a - T_w)] \quad (A.8)$$

Expanding and rearranging Eq. (A.8) gives

$$\frac{A}{g_b} = \rho_a c_p \frac{\Delta + \gamma}{\gamma}(T_s - T_w)$$

Finally, rearranging again, tree crown surface temperature can be given by

$$T_s = \frac{1}{\rho_a c_p}\frac{\gamma}{\Delta + \gamma}\frac{A}{g_b} + T_w$$

allowing surface temperature to be expressed in terms of available energy, aerodynamic conductance and wet bulb temperature of the air.

REFERENCES

Allen, M.B., Isaacson, E.L., 1998. Numerical Analysis for Applied Science. Wiley Series in Pure and Applied Mathematics, 1st ed. John Wiley & Sons, New York, USA, 492 pp.

Alves, I., Fontes, J.C., Pereira, L.S., 2000. Evapotranspiration estimation from infrared surface temperature. II. The surface temperature as a wet bulb temperature. Transactions of the ASAE 43 (3), 599–602.

Angelocci, L.R., Nova, N.A.V., Filho, M.A.C., Marin, F.R., 2004. Measurements of net radiation absorbed by isolated acid lime trees (*Citrus latifolia* Tanaka). Journal of Horticultural Science and Biotechnology 79 (5), 699–703.

Asdak, C., Jarvis, P.G., Gardingen, P.V., 1998. Modelling rainfall interception in unlogged and logged forest areas of Central Kalimantan, Indonesia. Hydrology and Earth System Sciences 2 (2–3), 211–220.

Beer, T., 1990. Applied Environmetrics Meteorological Tables. Applied Environmetrics, Victoria, 56 pp.

Bindon, H.H., 1965. A critical review of tables and charts used in psychrometry. In: Ruskin, R.E. (Ed.), Principles and Methods of Measuring Humidity in Gases, Humidity and Moisture—Measurement and Control in Science and Industry. Reinhold Publishing Corporation, New York, pp. 3–15.

Brenner, A.J., Jarvis, P.G., 1995. A heated leaf replica technique for determination of leaf boundary layer conductance in the field. Agricultural and Forest Meteorology 72, 261–275.

Brutsaert, W., 1991. Evaporation into the Atmosphere. Environmental Fluid Mechanics. Kluwer Academic Publishers, Dordrecht, The Netherlands, 299 pp.

Carlyle-Moses, D.E., Price, A.G., 1999. An evaluation of the Gash interception model in a northern hardwood stand. Journal of Hydrology 214, 103–110.

Carreiras, J.M.B., Pereira, J.M.C., Pereira, J.S., 2006. Estimation of tree canopy cover in evergreen oak woodlands using remote sensing. Forest Ecology and Management 223, 45–53.

Chen, J.M., Ibbetson, A., Milford, J.R., 1988a. Boundary-layer resistances of artificial leaves in turbulent air. II. Leaves inclined to the mean flow. Boundary-Layer Meteorology 45 (4), 371–390.

Chen, J.M., Ibbetson, A., Milford, J.R., 1988b. Boundary-layer resistances of artificial leaves in turbulent air. I. Leaves parallel to the mean flow. Boundary-Layer Meteorology 45 (1–2), 137–156.

Colley, S.J., 1998. Vector Calculus. Prentice-Hall, Inc., New Jersey.

Dalton, J., 1802. On evaporation. In: Gash, J.H.C., Shuttleworth, W.J. (Eds.), Evaporation, Benchmark Papers in Hydrology. IAHS Press, Wallingford, pp. 121–141.

Daudet, F.A., Le Roux, X., Sinoquet, H., Adam, B., 1999. Wind speed and leaf boundary layer conductance variation within tree crown: consequences on leaf-to-atmosphere coupling and tree functions. Agricultural and Forest Meteorology 97 (3), 171–185.

David, J.S., Valente, F., Gash, J.H.C., 2005. Evaporation of intercepted rainfall. In: Anderson, M.G. (Ed.), Encyclopedia of Hydrological Sciences. John Wiley & Sons Ltd., Chichester, UK, (Chapter 43), pp. 627–634.

David, T.S., Ferreira, M.I., Cohen, S., Pereira, J.S., David, J.S., 2004. Constraints on transpiration from an evergreen oak tree in southern Portugal. Agricultural and Forest Meteorology 122 (3–4), 193–205.

David, T.S., Gash, J.H.C., Valente, F., Pereira, J.S., Ferreira, M.I., David, J.S., 2006. Rainfall interception by an isolated evergreen oak tree in a Mediterranean savannah. Hydrological Processes 20 (13), 2713–2726.

Dolman, A.J., 1993. A multiple-source land surface energy balance model for use in general circulation models. Agricultural and Forest Meteorology 65, 21–45.

Domingo, F., Gardingen, P.R.V., Brenner, A.J., 1996. Leaf boundary layer conductance of two native species in southeast Spain. Agricultural and Forest Meteorology 81, 179–199.

Forgeard, F., Gloaguen, Y.C., Touffet, J., 1980. Interception des précipitations et apport au sol d'éléments minéraux par les

eaux de pluie et les pluviolessivats dans une hêtraie atlantique et dans quelques peuplements résineux en Bretagne. Annales des Sciences Forestières 37, 53–71.
Gash, J.H.C., 1979. An analytical model of rainfall interception by forests. Quarterly Journal of the Royal Meteorological Society 105, 43–55.
Gash, J.H.C., Lloyd, C.R., Lachaud, G., 1995. Estimating sparse forest rainfall interception with an analytical model. Journal of Hydrology 170, 79–86.
Gash, J.H.C., Shuttleworth, W.J. (Eds.), 2007. Evaporation, Benchmark Papers in Hydrology, vol. 2. IAHS Press, Wallingford, pp. 521.
Gash, J.H.C., Valente, F., David, J.S., 1999. Estimates and measurements of evaporation from wet, sparse pine forest in Portugal. Agricultural and Forest Meteorology 94, 149–158.
Grace, J., 1983. Plant–Atmosphere Relationships. Outline Studies in Ecology. Chapman and Hall Ltd., New York, 92 pp.
Grace, J., Fasehun, F.E., Dixon, M., 1980. Boundary layer conductance of the leaves of some tropical timber trees. Plant, Cell and Environment 3 (6), 443–450.
Grantz, D.A., Vaughn, D.L., 1999. Vertical profiles of boundary layer conductance and wind speed in a cotton canopy measured with heated brass surrogate leaves. Agricultural and Forest Meteorology 97 (3), 187–197.
Hall, R.L., 2002. Aerodynamic resistance of coppiced poplar. Agricultural and Forest Meteorology 114, 83–102.
Herbst, M., Roberts, J.M., Rosier, P.T.W., Gowing, D.J., 2006. Measuring and modelling the rainfall interception loss by hedgerows in southern England. Agricultural and Forest Meteorology 141 (2–4), 244–256.
INMG, 1991. Normais climatológicas da região de ''Alentejo e Algarve'', correspondentes a 1951-1980. O Clima de Portugal, Fascículo XLIX - Volume 4 - 4a Região. INMG - Instituto Nacional de Meteorologia e Geofísica, Lisboa, 98 pp.
Jackson, N.A., 2000. Measured and modelled rainfall interception loss from an agroforestry system in Kenya. Agricultural and Forest Meteorology 100, 323–336.
Jones, H.G., 1992. Plants and Microclimate, 2nd ed. Cambridge University Press, Cambridge, 428 pp.
Kutner, M.H., Nachtsheim, C.J., Neter, J., Li, W., 2005. Applied Linear Statistical Models, 5th ed. McGraw-Hill Higher Education, 1424 pp.
Landsberg, J.J., Powell, D.B.B., 1973. Surface exchange characteristics of leaves subject to mutual interference. Agricultural Meteorology 12, 169–184.
Landsberg, J.J., Thom, A.S., 1971. Aerodynamic properties of a plant of complex structure. Quarterly Journal of the Royal Meteorological Society 97, 565–570.
Lankreijer, H.J.M., Hendriks, M.J., Klaassen, W., 1993. A comparison of models simulating rainfall interception of forests. Agricultural and Forest Meteorology 64 (3–4), 187–199.
Lloyd, C.R., Gash, J.H.C., Shuttleworth, W.J., de O Marques, F.A., 1988. The measurement and modelling of rainfall interception by Amazonian rain forest. Agricultural and Forest Meteorology 43 (3–4), 277–294.
McNaughton, K.G., Green, S.R., Black, T.A., Tynan, B.R., Edwards, W.R.N., 1992. Direct measurement of net radiation and photosynthetically active radiation absorbed by a single tree. Agricultural and Forest Meteorology 62, 87–107.
Michaletz, S.T., Johnson, E.A., 2006. Foliage influences forced convection heat transfer in conifer branches and buds. New Phytologist 170 (1), 87–98.
Monteith, J.L., 1965. Evaporation and environment. In: Gash, J.H.C., Shuttleworth, W.J. (Eds.), Evaporation, Benchmark Papers in Hydrology. IAHS Press, Wallingford, pp. 337–366.
Monteith, J.L., Unsworth, M.H., 2008. Principles of Environmental Physics, 3rd ed. Academic Press, London, 418 pp.
Moore, C.J., Fisch, G., 1986. Estimating heat storage in Amazonian tropical forest. Agricultural and Forest Meteorology 38 (1–3), 147–168.
Penman, H.L., 1948. Natural evaporation from open water, bare soil and grass. In: Gash, J.H.C., Shuttleworth, W.J. (Eds.), Evaporation, Benchmark Papers in Hydrology. IAHS Press, Wallingford, pp. 186–212.
Pereira, F.L., Gash, J.H.C., David, J.S., David, T.S., Monteiro, P.R., Valente, F., 2009. Modelling interception loss from evergreen oak Mediterranean savannas. Application of a tree-based modelling approach. Agricultural and Forest Meteorology 149, 680–688.
Pereira, J.S., Mateus, J.A., Aires, L.M., Pita, G., Pio, C., David, J.S., Andrade, V., Banza, J., David, T.S., Paço, T.A., Rodrigues, A., 2007. Net ecosystem carbon exchange in three contrasting Mediterranean ecosystems—the effect of drought. Biogeosciences 4 (5), 791–802.
R Development Core Team, 2007. R: A Language and Environment for Statistical Computing. R Foundation for Statistical Computing, Vienna, Austria.
Ross, J., 1975. Radiative transfer in plant communities. In: Monteith, J.L. (Ed.), Vegetation and the Atmosphere. Academic Press, London, pp. 13–56.
Rutter, A.J., Robins, P.C., Morton, A.J., Kershaw, K.A., 1971. A predictive model of rainfall interception in forests. 1. Derivation of the model from observations in a plantation of Corsican pine. Agricultural Meteorology 9, 367–384.
Schuepp, P.H., 1993. Leaf Boundary-Layers. New Phytologist 125 (3), 477–507 (Tansley Review No. 59).
Shuttleworth, W.J., Wallace, J.S., 1985. Evaporation from sparse crops—an energy combination theory. Quarterly Journal of the Royal Meteorological Society 111, 839–855.
Smith, D.M., Jarvis, P.G., Odongo, J.C.W., 1997a. Aerodynamic conductances of trees in windbreaks. Agricultural and Forest Meteorology 86, 17–31.
Smith, D.M., Jarvis, P.G., Odongo, J.C.W., 1997b. Energy budgets of windbreak canopies in the Sahel. Agricultural and Forest Meteorology 86 (1–2), 33–49.
Stewart, J.B., 2004. Review of forest evaporation studies, primarily in the United Kingdom. In: Mencuccini, M., Grace, J., Moncrieff, J., McNaughton, K.G. (Eds.), Forests at the Land–Atmosphere Interface. CAB International, Edinburgh, UK, pp. 159–174.
Stewart, J.B., Thom, A.S., 1973. Energy budgets in pine forest. Quarterly Journal of the Royal Meteorological Society 99 (419), 154–170.
Stokes, V.J., Morecroft, M.D., Morison, J.I.L., 2006. Boundary layer conductance for contrasting leaf shapes in a deciduous broadleaved forest canopy. Agricultural and Forest Meteorology 139 (1–2), 40–54.
Teklehaimanot, Z., Jarvis, P.G., 1991. Direct measurement of evaporation of intercepted water from forest canopies. Journal of Applied Ecology 28 (2), 603.
Teklehaimanot, Z., Jarvis, P.G., Ledger, D.C., 1991. Rainfall interception and boundary layer conductance in relation to tree spacing. Journal of Hydrology 123, 261–278.
Thom, A.S., 1975. Momentum, mass and heat exchange of plant communities. In: Monteith, J.L. (Ed.), Vegetation and the Atmosphere. Academic Press, London, pp. 57–110.
Thorpe, M.R., 1978. Net radiation and transpiration of apple trees in rows. Agricultural Meteorology 19 (1), 41–57.
Thorpe, M.R., Butler, D.R., 1977. Heat transfer coefficients for leaves on orchard apple trees. Boundary-Layer Meteorology 12 (1), 61–73.
Valente, F., David, J.S., Gash, J.H.C., 1997. Modelling interception loss for two sparse eucalypt and pine forests in central

Portugal using reformulated Rutter and Gash analytical models. Journal of Hydrology 190, 141–162.
Wright, I.R., Gash, J.H.C., Rocha, H.R.D., Shuttleworth, W.J., Nobre, C.A., Maitelli, G.T., Zamparoni, C.A.G.P, Carvalho, P.R.A., 1992. Dry season micrometeorology of central Amazonian ranchland. Quarterly Journal of the Royal Meteorological Society 118, 1083–1099.
Wünsche, J.N., Lakso, A.N., Robinson, L., 1995. Comparison of four methods for estimating total light interception by apple trees of varying forms. Horticultural Science 30 (2), 272–276.